AGU ADVANCING EARTH AND SPACE SCIENCES

Geophysical Research Letters®

RESEARCH LETTER
10.1029/2023GL106284

Slow Dynamics of Hydrate Systems Revealed by a Double BSR

M. Fabre[1,2], V. Riboulot[1], L. Loncke[2], S. Ker[1], G. Ballas[3], Y. Thomas[1], G. Ion[4], and N. Sultan[1]

[1]Geo-Ocean, Université de Brest, CNRS, Ifremer, Plouzané, France, [2]CEFREM, Université de Perpignan Via Domitia, Perpignan, France, [3]Geosciences Montpellier, Université de Montpellier, CNRS, Montpellier, France, [4]GeoEcoMar, Bucharest, Romania

Key Points:

- A 2D modeling reveals the observed deeper secondary BSR is mostly consistent with a paleo-BSR developed during the last glacial period
- A paleo-BSR can only be preserved in sediments if the period of stagnation of the base of hydrate layers is sufficient to trap enough gas
- Although rapid environmental changes, the hydrate-free gas system reacts much more slowly preventing catastrophic submarine destabilization

Supporting Information:

Supporting Information may be found in the online version of this article.

Correspondence to:

M. Fabre,
maud.fabre@ifremer.fr

Citation:

Fabre, M., Riboulot, V., Loncke, L., Ker, S., Ballas, G., Thomas, Y., et al. (2024). Slow dynamics of hydrate systems revealed by a double BSR. *Geophysical Research Letters*, *51*, e2023GL106284. https://doi.org/10.1029/2023GL106284

Received 15 NOV 2023
Accepted 5 MAR 2024

Author Contributions:

Conceptualization: V. Riboulot, L. Loncke, N. Sultan
Data curation: M. Fabre, V. Riboulot, S. Ker, Y. Thomas, N. Sultan
Formal analysis: M. Fabre
Funding acquisition: V. Riboulot
Investigation: M. Fabre
Methodology: M. Fabre, V. Riboulot, L. Loncke, G. Ballas, N. Sultan
Project administration: V. Riboulot, L. Loncke
Resources: V. Riboulot, L. Loncke, S. Ker, Y. Thomas, N. Sultan
Supervision: V. Riboulot, L. Loncke, N. Sultan
Visualization: M. Fabre

Abstract Determining how gas hydrate distribution evolved along continental margins in the past is essential to understanding its evolution in the future. Moreover, hydrate decomposition has been linked to several catastrophic events, including some of the largest submarine landslides on Earth and the massive release of greenhouse gases into the ocean. Offshore Romania, the presence of a second bottom-simulating reflector (BSR) provides an opportunity to gain valuable insights into hydrate dynamics since the Last Glacial Period (LGP). We conducted transient modeling of hydrate thermodynamic stability by merging in-situ observations with indirect assessments of sea-bottom temperature, thermal conductivity, salinity, sedimentation rate, and sea-level variations. We reveal a strong correlation between the BSRs and the base of the Gas Hydrate Stability Zone (GHSZ) during both the present and LGP periods. The gradual evolution of the GHSZ over the past 34 ka presented here supports a conceptual model that excludes catastrophic environmental scenarios.

Plain Language Summary Methane hydrate is an ice-like compound composed of a cage of water molecules enclosing a methane molecule. Hydrates can form in marine sediments along continental margins where water and methane are present under high pressure and low temperatures. As a result of climate change, hydrate melting has been linked to catastrophic events, including submarine landslides and the release of greenhouse gases into the ocean. Offshore Romania, the presence of a relic of the base of the hydrate layers formed in sediments during past glacial conditions, reveals the evolution of the hydrate stability zone since the last glacial period. The 2D modeling results have enabled us to define the area where hydrates alternately melt and reform in response to environmental changes such as rising temperatures and sea levels. Our results show that the evolution of gas-hydrate accumulations generates multiple, slow chain reactions, preventing the system from disastrous destabilization, sequentially provoking catastrophic events.

1. Introduction

Gas hydrates (GH) naturally store a considerable volume of methane in marine sediments where the pressure-temperature (P-T) conditions, pore-fluid salinity, and gas composition are among the main parameters controlling their stability (Sloan & Koh, 2007). Seaward shifts of GH stability conditions, leading to methane venting into the ocean are due to contemporary warming of bottom waters (e.g., Phrampus & Hornbach, 2012), sea level variations (e.g., Nisbet & Piper, 1998), and changes in salinity (Riboulot et al., 2018). So, climate changes can significantly impact the GHSZ (Andreassen et al., 2017; Davies et al., 2017). Conversly, methane from GH dissociation could be a potential greenhouse agent following the "*clathrate gun hypothesis*" (Kennett et al., 2003), and triggering hyperthermal maximum events across geological times (Dickens et al., 1997; Jahren et al., 2001). But, this contribution to the climate change remains debated (Ruppel & Kessler, 2017) and improved, constrained knowledge of hydrate dynamics following changes in environnemental conditions is necessary.

Evidence of GH in marine sediments can be inferred through the identification of a BSR in seismic data. Some BSRs occur at or close to the current Base of the GHSZ (BGHSZ) in response to the acoustic impedance contrast between GH accumulations and underlying trapped free gas (e.g., Somoza et al., 2022; Xu & Ruppel, 1999). Sometimes, more than one BSR can coexist (e.g., Davies et al., 2021; Popescu et al., 2006), due, for instance, to the layering of various gas compositions (Geletti & Busetti, 2011), or other diagenetic processes (Berndt et al., 2004; Somoza et al., 2022). But, changes in the GH stability field may result in the preservation of a certain amount of GH in a state of disequilibrium (e.g., due to water-temperature warming, re-equilibration of thermal gradients, or sea-level fluctuations, rapid sedimentation, tectonic uplift), implying migration process of the

Writing – original draft: M. Fabre
Writing – review & editing: V. Riboulot, L. Loncke, S. Ker, G. Ballas, G. Ion, N. Sultan

BGHSZ (Colin et al., 2020) and resulting in the formation of a paleo-BSR (Auguy et al., 2017; Posewang & Mienert, 1999). The insights into the existence of a paleo-BSR would be of crucial importance to assess the dynamics of the GHSZ after variations in environmental conditions. To verify this theory, we investigated the GH system of the western Black Sea (BS), where a large GH occurrence zone has been reported on the slope, supported by BSR on seismic data (Colin et al., 2020; Haeckel et al., 2015; Popescu et al., 2006, 2007; Vasilev et al., 2013) or by sampling (Yefremova, and Zhizchenko, 1974; Riedel et al., 2020), as well as an active gas flare area located upslope of it (e.g., Riboulot et al., 2017) (Figure 1).

During its recent geological history (the late Quaternary Period), the BS was totally disconnected from the world oceans (Major et al., 2006; Soulet et al., 2011). This long-term isolation induced a drastic change in the BS water salinity (Soulet et al., 2010) and modified the sediment pore water salinity and therefore, the hydrate equilibrium conditions (Sloan & Koh, 2007). Prior to the reconnection of the BS with the Mediterranean Sea at approximately 9,000 calendar year before present (9 Kyr cal BP), the BS evolved as a fresh to brackish water lake with a water characterized by a salt concentration of 2 psu (Practical Salinity Unit) and a sea bottom temperature of ∼4°C (Soulet et al., 2010). During the reconnection, via the Bosphorus Strait (Figure 1a), hydrological changes were drastic. Consequently, the sea bottom water warmed up to the current conditions at 8.9°C (Riboulot et al., 2017) and bottom water salinities increased up from a couple of psu to ∼22 psu and remained stable for the last 2,500 years of the reconnection (Soulet et al., 2010).

In this context, we addressed three key points related to this system by: (a) assessing the nature of a second BSR observed in the investigated zone, close to an area where Popescu et al. (2006) have already evidenced the presence of five stacked BSRs (b) defining how the GHSZ evolves over time and space and (c) determining why a second BSR still imprints the sediments.

Based on exhaustive knowledge on the hydrological and thermal conditions of the BS, and on new chronostratigraphic constrains from Martinez-Lamas et al. (2020) informing about the seafloors evolution since the last 33.5 ka in the study zone, we tested the dynamic response of the GH to the environmental changes which have characterized the western BS since the end of the LGP. This was performed by dynamic 2D multi-parametric modeling allowing to assess past positions of the BGHSZ through time and compare them with the observed secondary BSR.

2. Results

2.1. The Double BSR, Geophysical Observations and Characterization

High-resolution seismic lines (GHASS cruise (2015); https://doi.org/10.17882/96701, Thomas et al., 2023; see section Text S1 and Figure S1 in Supporting Information S1) reveal the presence of two stacked BSRs in the study area (Figure 2a). The primary, shallower BSR (BSR1), and the secondary, deeper (BSR2), cross cut stratigraphic layers and mimic the seafloor, while exhibiting a polarity reversal. Their positions can be identified through aligned amplitude terminations (Colin et al., 2020), and by the presence of both attenuation of high frequencies and lower velocity below the distinct BSRs (Figures 3 and 4). BSR2 is patchy, 130 m beneath the BSR1, weaker in amplitude in comparison with BSR1 and attenuation is stronger under BSR2.

BSR2 is amplified along two well-defined patches: (a) seaward, BSR2 is parallel and located 130 m below BSR1 (Figures 2a(b) and 2a(c)); (b) landward, a second patch, is characterized by aligned high amplitude terminations (Figures 2a(d) and detailed view in Figure S1B in Supporting Information S1). This patch exhibits a highly incurved shape that mimics an old head-scarp, which still imprints the current slope morphology (Figure 1).

The upper limits of BSR1 and BSR2 show distinct pinch-out on the seafloor (Figure 2a). The landward termination of BSR1 was detected down to 660 m water depth (projection on present-day bathymetry). However, we lose track of it above 25 mbsf. The termination of BSR2 is most perceptible at the extremity of the landward segment (Figure S1B in Supporting Information S1), which reaches almost 520 m water depth (projection on present-day bathymetry). We lose track of it at 50 mbsf (Figures 2a(d)).

The amplitude section of the HR reference profile highlights high-amplitude reflections below the two BSRs, particularly enhanced below the BSR1, indicating varying free-gas concentrations (Figure 3a). We notice lateral amplitude variations along the BSR particularly expressed along the BSR1 reflector; highest amplitudes exist where faults cross-cut the stratification and BSR2. The variation of signal frequency content can be used to

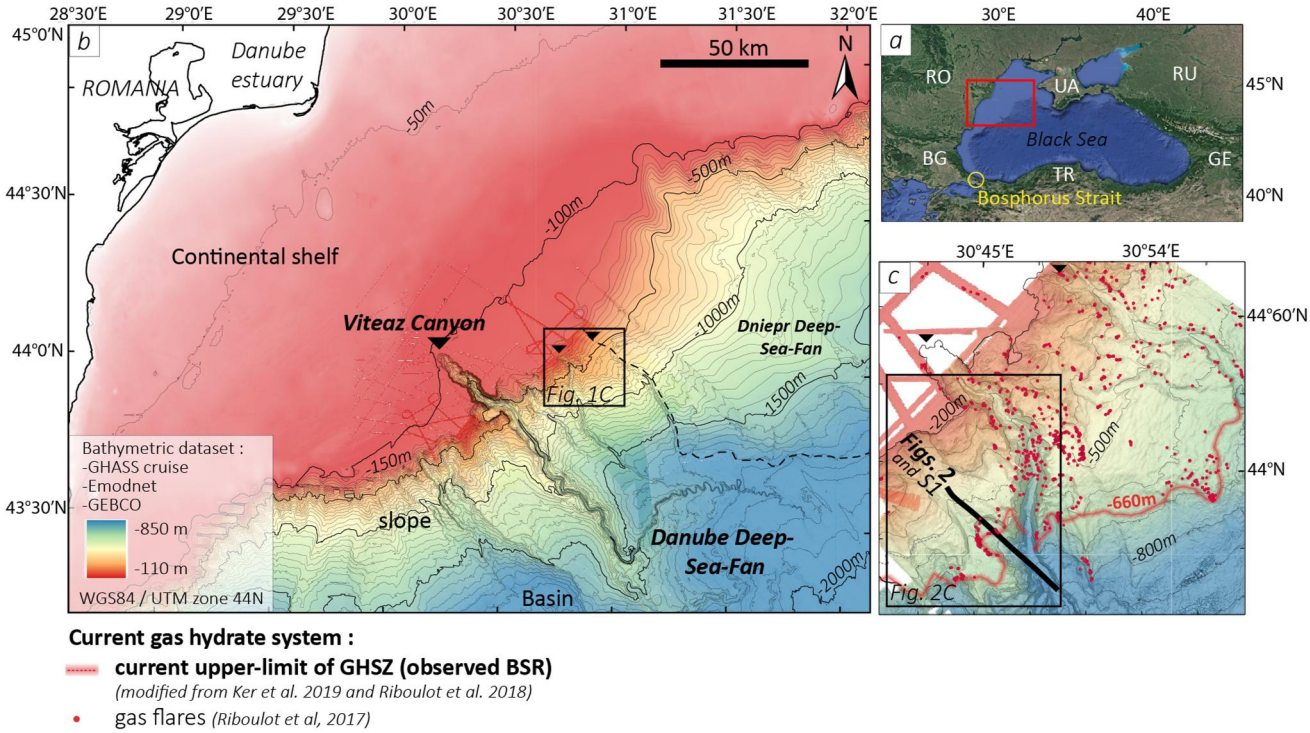

Figure 1. (a) General view of the BS (b) Bathymetric map of the western BS (c) Morphology and detailed features characterizing the study zone. The bold black line represents the location of seismic lines presented in Figure 2 and S1 in Supporting Information S1.

evidence the presence of seismic attenuation due to the presence of free gas. Focusing on the second BSR, Figure 3b shows a threshold effect at both BSR interfaces, expressed by an attenuation of high frequencies below the distinct BSRs, particularly stronger under BSR2. Such an effect on the amount of seismic attenuation can be due to the presence of low-density fluids in the sediment (Anderson & Bryant, 1990; Ruppel et al., 2005), and indicates in our case that high concentrations of free gas are still present under BSR2.

Velocity analysis was performed every 150 m laterally, permitting to compare the depth-converted seismic section with the velocity field (Figure 4). It shows varying velocity in sediments (1,470–1,950 m/s), and particularly lower values below BSR1 and BSR2. An inversion of the velocity below BSR2, combined with the persistence of high impedance contrast at the BSRs interfaces and the attenuation of high frequency (Figure 3b), support the hypothesis of the presence of excess free gas in sediments below the BSR2. The lower velocity under BSR2, suggests higher concentrations of free gas below BSR2 in comparison with BSR1. Lastly, a local rapid gas migration process through observed faults (in contrast with the long-lasting gas diffusion process in sediments) could explain high free gas concentration below BSR1, and the low velocity zone.

2.2. Spatio-Temporal Modeling of the GHSZ Since the Last −34 ka

We calculated the depths of phase equilibria of GH at different time steps based on ongoing environmental parameters. For the 34,000-year-period calculations, a dynamic 2D multi-parametric GH stability model developed by Sultan et al. (2010) was used to simulate the evolution of the GHSZ. Modeling was performed using the NW-SE depth-converted seismic HR profile presented in Figure 2 with a time step of 1 year for each calculation. Further details on modeling inputs and the scenarios tested are reported in sections *Modeling Method* (Text S2, Figures S2, S3, S4, S5 in Supporting Information S1) and *Tested scenarios* (Text S3, Table S1 in Supporting Information S1) in Supporting Information.

All modeling results (Figures S6 and S7 in Supporting Information S1) predict consistent general patterns specifically showing a seaward migration trend of the GHSZ between −33.5 ka and the present-day (Figure 2b). During the LGP, the GHSZ calculated between −33.5 and −20 ka (purple envelope, Figure 2b), remains stable, and the upper limit of the GHSZ extended from ~495 m ±5–525 m ±5 water-depth (projected on present-day

10.1029/2023GL106284

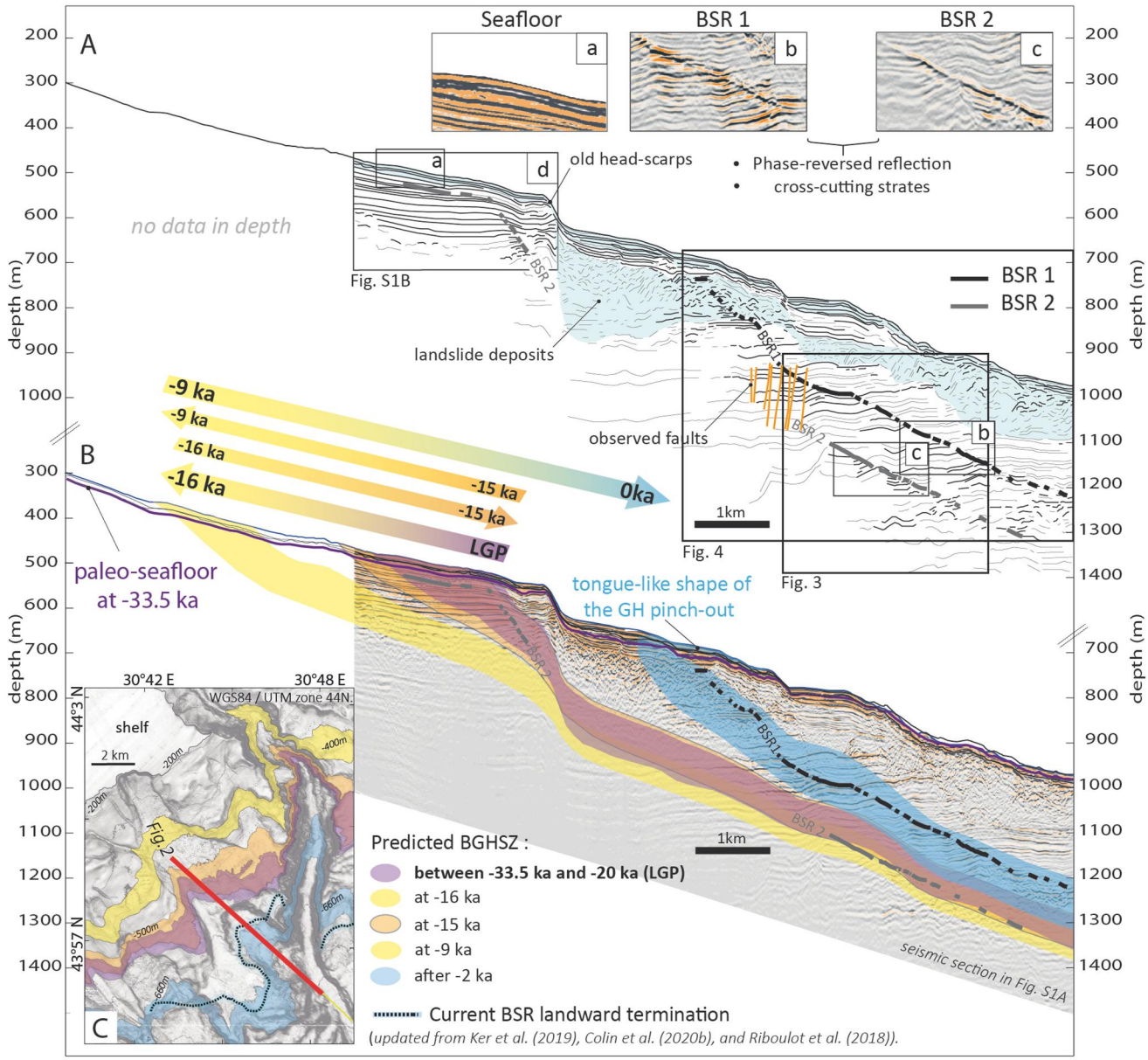

Figure 2. (a) Depth converted HR seismic profile showing two BSRs along the study area. The reflection of BSRs (insets b, c) presents a polarity reversal compared to the seafloor (inset a). Inset d is shown in Figure S1B in Supporting Information S1 (b) Modeling results are calculated from different scenarios (Figures S2, S6, S7 and Table S1 in Supporting Information S1). Each envelope represents the positions of BGHSZ computed at different time ranges (colored arrows provide information on the general trend of GHSZ since the LGP) and results from computed modeling results detailed in Figures S6 and S7 in Supporting Information S1 (c) Modeled GHSZ pinch outs are reported on the bathymetric map.

seafloor). The modeling results show strong correlation with the position of BSR2, particularly along its two expressed patches in seismic data (Figures 2a(b) and 2a(d)).

After −20 ka, the modeling results show a sudden back-and-forth movement of the GHSZ upper limit along the slope. This is illustrated by an upward displacement (yellow envelope Figure 2b) in response to a sea-level rise of ≤+100 m at −16 ka, before returning to its LGP position at −15 ka (orange envelope, Figure 2b) due to a sea-level drop episode (Figure S2A in Supporting Information S1). This was followed by a landward extension of the GHSZ reaching its maximum extent at −9 ka (again yellow envelope, Figure 2b), in response to the last sea-level rise.

After −9 ka, the extension of the GHSZ drastically decreased due to the warming and re-salinization of the BS. Simultaneously, the thickness of the GH layer decreased by 130 m caused by the upward migration of the BGHSZ

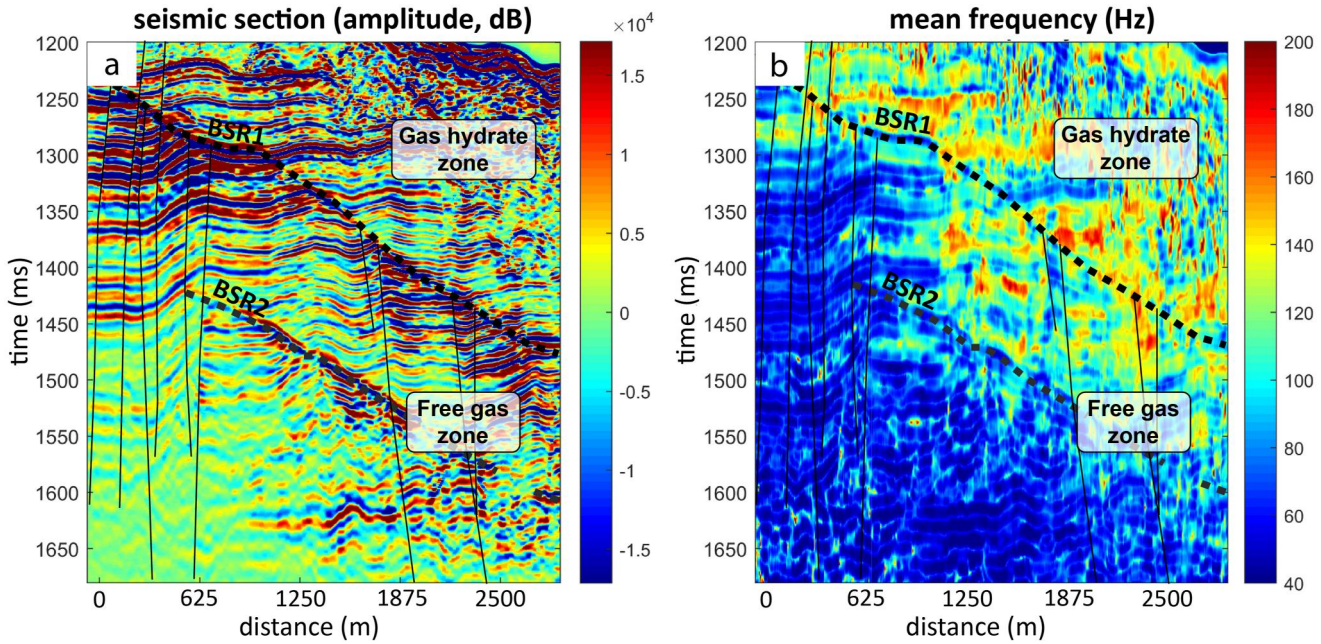

Figure 3. Geophysical characterization of the two BSRs on the presented high-resolution seismic profile (Figure 2). (a) Amplitude section (b) mean frequency section. Observed faults appear along thin black lines. Location of the sections is reported on Figure 2a.

(blue envelope, Figure 2b). The predicted present-day GHSZ reaches its termination close to the seafloor at 660 m water depth, delimiting the current upper limit of the GHSZ which fits well with BSR1. It displays a tongue-like shape at the GH pinch-out (Figure 2b), which expresses GH decomposition near the seafloor in response to the progressive diffusion of salt within the sediment (Riboulot et al., 2018).

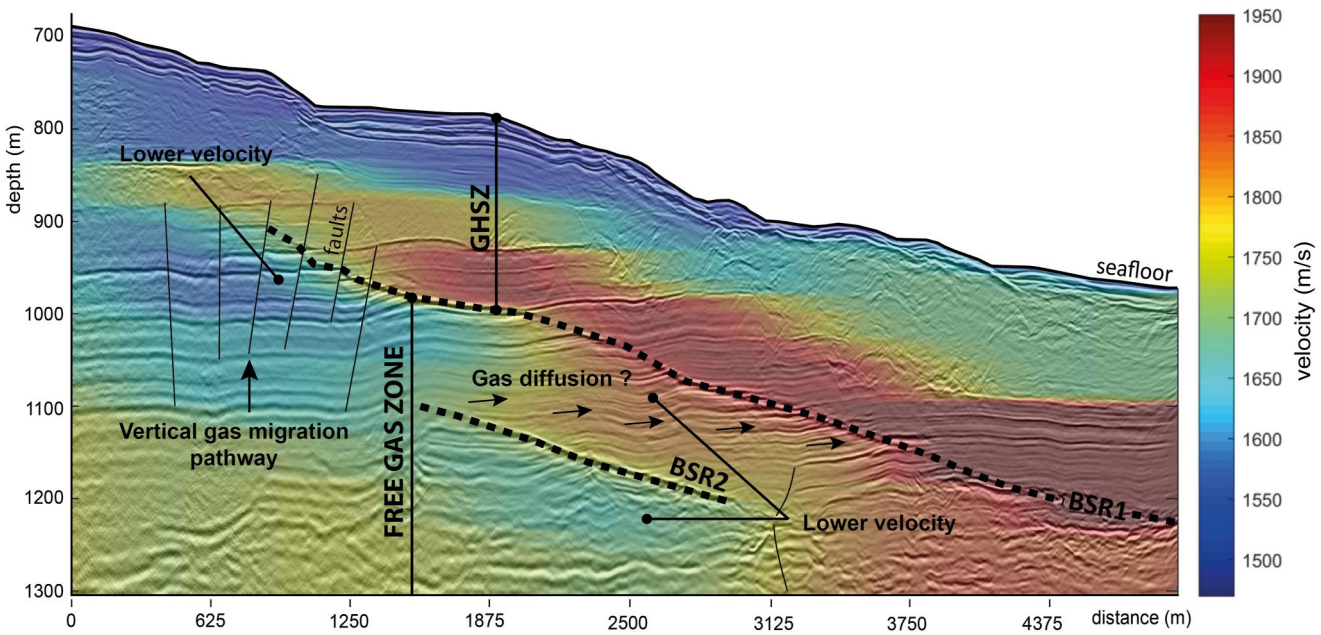

Figure 4. Overlay of depth-converted seismic section and velocity model performed every 150 m corresponding to the lateral resolution of the resulting velocity field. Details on the velocity decrease at the two BSR interfaces (inversion). Lower velocity was identified below the two BSRs, particularly well pronounced under BSR2, suggesting high concentrations of free gas in sediments. The faults (black thin lines) have been represented to evidence their role on the migration process (black arrows) and the consequence on the velocity field. GHSZ: Gas Hydrate Stability Zone. Location of the sections is reported on Figure 2a.

3. Discussion

3.1. Origin of the Double BSR

In the study area, BSR1 represents the current BGHSZ (Popescu et al., 2006). BSR2 is more questionable. As below BSR1, the presence of low-velocity zones beneath BSR2 (Figure 4) indicates the existence of free gas beneath this reflector, clearly differentiating it from a diagenetic opal-A/opal-CT BSR (Berndt et al., 2004) or smectite-illite BSR (Srodon & Eberl, 1984).

Instead, along continental margins, a double BSR can be theoretically explained by the following distinct hypotheses: (a) the presence of GH with a distinct gas composition, (b) a former position of the BGHSZ. The tectonic uplift in relation to subduction processes, as a mechanism for the formation of a double BSR (Han et al., 2021), can be ruled out of the discussion.

3.1.1. Distinct Gas Composition Hypothesis

Multiple BSRs can represent the bases of successive layers of GH with distinct compositions. The presence of a mixture of gases could explain the existence of two BSRs as a deeper GHSZ as demonstrated worldwide (Geletti & Busetti, 2011; Posewang & Mienert, 1999). In the study area, the composition of the hydrate-forming gas at BSR1 offshore Romania is 99.6% methane of microbial origin as demonstrated by sampling (Riboulot et al., 2018) and geochemical analysis (Riedel et al., 2020). Thermogenic sources have also been detected offshore Crimea but far from the study area (Starostenko et al., 2010).

3.1.2. Paleo-BSR Hypothesis

Alternatively, stacked BSRs could represent relics of former positions of the BGHSZ which can be regarded as potential frozen proofs of environmental conditions for distinct cold climatic episodes (Bangs et al., 2005; Davies et al., 2021; Popescu et al., 2006). Our modeling provides new insights by demonstrating that BSR2 correlates with the position of the BGHSZ at the LGP when BS was a freshwater lake. Its landward termination seems to pinch just under a reflector dated back to 33.5 ka by Martinez-Lamas et al. (2020), considered as the paleo-seafloor calculated for the LGP (Figure S5 in Supporting Information S1).

Between −33.5 ka to −20 ka, the GHSZ appears to be spatially stable (Figure 2b), suggesting it was thermodynamically in steady state for at least 13.5 ka (Figures 5(1)). Then, the positions of predicted BGHSZ migrated over time, probably punctuated by alternating GH recrystallization (Figures 5(2 and 4)) and dissociation processes in sediment (Figures 5(3 and 5)). This reveals that the GH was highly sensitive to the sea-level fluctuations that characterized the BS before −9 ka, demonstrating a strong response of the GHSZ to two episodes of sea-level rise (Figures 5(2–4). This sensitivity led to a back-and-forth movement of the narrowest upper part of the GHSZ along the slope which may have acted as a buffer zone. The effect of salinity and temperature diffusion clearly prevailed after −9 ka to present as evidenced by the upward migration of the BGHSZ from the BSR2 to the BSR1 position. This migration was accompanied by a reduction in the extension of the GHSZ which occurred more or less progressively depending on the scenario of sea-bottom temperature re-equilibration (Figures 5(5), S2b and S6 in Supporting Information S1).

3.2. Preservation of a Paleo-BSR

One of the reasons why a paleo-BSR still imprints within sediments could be the effect of diagenetic processes (Posewang & Mienert, 1999) due to physical changes of bearing sediments at the exact position of old BGHSZ (Nimblett & Ruppel, 2003, and references therein). However, this hypothesis alone cannot explain the geophysical signature of BSR2 characterized by a polarity reversal (Figures 2a(c)), lower velocity and a larger attenuation of high frequencies below the BSR2 interface (Figures 3b and 4). These characteristics could be explained by a higher concentration of free gas under the old BGHSZ leading to the persistence of a negative acoustic impedance contrast at the BSR2 (Auguy et al., 2017).

In response to environmental changes, the re-equilibration of the old BGHSZ from BSR2 to its current position suggests a decomposition of GH in a mixture of free gas and dissolved gas in the GH destabilization zone (GHDZ) (Sultan, 2007) (Figures 5(5)). Experimental studies show that grain size and connectivity between microstructures of the host sediment determine how gas is transported toward the surface (Jain & Juanes, 2009;

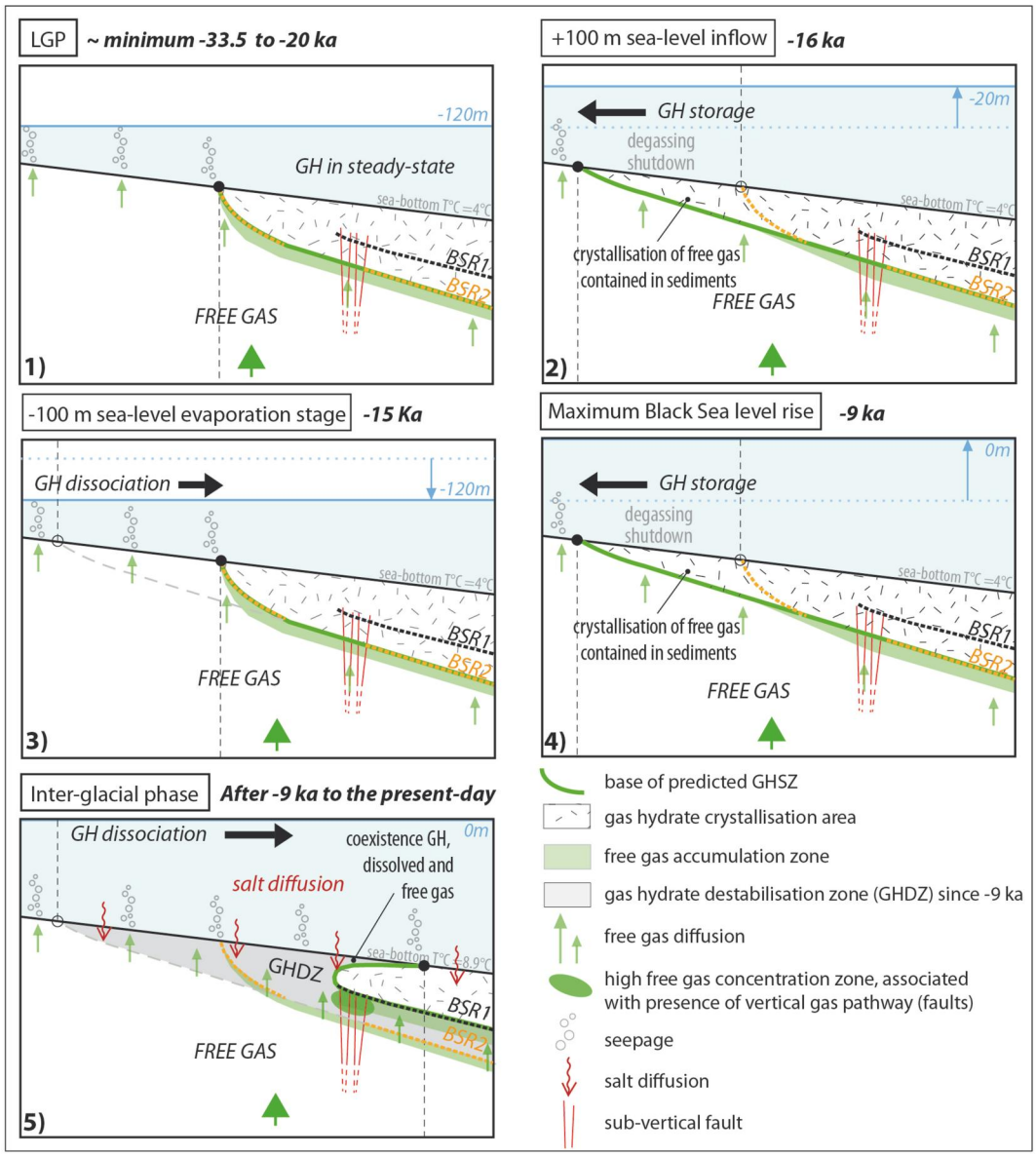

Figure 5. 2D conceptual scenario of the GHSZ evolution since the LGP in distinct steps (1–5), compared to the position of two observed BSRs. This study highlights the control of GH distribution by environmental changes and the associated gas diffusion process (green arrows) which governs free gas accumulation zones (in green). In the free gas domain (white zone) excess free gas is trapped below the BGHSZ which hampered vertical fluid migration.

Plaza-Faverola et al., 2023). In the study zone, the very low permeability of the host sediment containing high amounts of clay-silt (Ballas et al., 2018; Riedel et al., 2020) suggests that the fluid flow regime induced by hydrate dynamics is dominated by a gas diffusion process.

Locally, the presence of isolated sets of faults may provide gas migration pathways between the two BSRs (Figure 2a), suggesting that advection through discontinuities related to local excess pore pressure below the BSR2 is a mechanism that cannot be ruled out, particularly during GH dissociation (Figures 5(5)). A vertical gas migration from BSR2 to BSR1 though faults could explain the patchy geometry of BSR2, and the heterogeneous distribution of gas concentration detected below BSR2 (Figures 2a and 3a).

3.3. Why Only One Preserved Paleo-BSR?

The modeling results reveal more BGHSZ positions over time than observed BSRs in seismic data. The most likely explanation would be the time the BGHSZ spent at given positions. By examining the position of the BGHSZ over time, the position of BSR2 fits with the paleo-BGHSZ during the longest steady-state period (33,5–20 ka time frame), suggesting a significant accumulation of gas during this phase of stagnation to form BSR2 (Figures 5(1)).

The long-lasting process of gas diffusion in sediment has already been proposed by Ker et al. (2019) and Colin et al. (2020) in the study zone, due to the conjunction of low permeability in fine-grained sediment, and the process of hydrate re-crystallisation during decomposition, which can slow down the dissipation process below the BGHSZ (Sultan, 2007).

Accordingly, in contrast with the stable lowstand LGP period, we suppose that the fast migration of the BGHSZ that occurred between −20 ka and −9 ka (Figures 5(2–4)), most probably compromised the formation of a homogenous GH layer in view of the low gas volumetric concentrations of 4%–6% in the sediment (Ker et al., 2019), and prevented free-gas accumulations under the successive BGHZs to preserve another paleo-BSR.

4. Implications

This is the first attempt to model the evolution of the GHSZ with a short time step calculation applied here to the western BS since the LGP, where GH dynamics is difficult to consider due to the complexity and debated evolution scenarios of paleo-environmental conditions. Our modeling results show that the observed deeper secondary BSR is mostly consistent with a paleo-BSR that developed during LGP. Geophysical analysis shows that this paleo-BSR is still trapping free gas in depth. A slow gas diffusion rate coupled with likely diagenetic transformation of host sediments and the duration of the stagnation of BGHSZ over time is the most likely explanation for the preservation of a unique LGP paleo-BSR.

More generally, in GH systems where gas diffusion in sediment dominates, the long-lasting migration mechanism following environmental changes and associated hydrate dissociation leads us to minimize the catastrophist *Clathrate gun* hypothesis (Kennett et al., 2003), which argues for a massive gas emission directly into the ocean, and a predisposition of slope sediment instabilities. We now understand that the release of methane during a hydrate dissociation phase is slow due to the overpressure generated by their decomposition leading to re-crystallization (Colin et al., 2020; Ker et al., 2019) and the slow gas diffusion process in clayey sediments. Although environmental changes can be rapid as observed in the BS since the LGP, the hydrate-free gas system reacts much more slowly preventing any catastrophic destabilization.

Data Availability Statement

The seismic data (depth migrated seismic profile) and the velocity model used for the study will be available using the repository SeaNoe via a doi identifier link (https://doi.org/10.17882/96701, Thomas et al., 2023). All the files relative to the model calculations and modeling results will be available using the Zenodo repository (https://doi.org/10.5281/zenodo.8417400, Fabre, 2023).

Acknowledgments
The support by officers and crew during the GHASS cruise (2015–10.17600/15000500) and GHASS2 (2021–10.17600/18001358) on board R/V Pourquoi Pas? Was greatly appreciated, as is the dedication of the Genavir and Ifremer technical staff during the cruise. We thank A. Chalm from IFREMER for revision of the English language. This work was funded by the BLAME project sponsored by the French National Research Agency (ANR-18-CE01-0007) and supported by the CEFREM laboratory of University of Perpignan, and the scientific consortium Geo-Ocean UMR6538.

References

Anderson, A. L., & Bryant, W. R. (1990). Gassy sediment occurrence and properties: Northern Gulf of Mexico. *Geo-Marine Letters*, *10*(4), 209–220. https://doi.org/10.1007/bf02431067

Andreassen, K., Hubbard, A., Winsborrow, M., Patton, H., Vadakkepuliyambatta, S., Plaza-Faverola, A., et al. (2017). Massive blow-out craters formed by hydrate-controlled methane expulsion from the Arctic seafloor. *Science*, *356*(6341), 948–953. https://doi.org/10.1126/science.aal4500

Auguy, C., Calvès, G., Calderon, Y., & Brusset, S. (2017). Seismic evidence of gas hydrates, multiple BSRs and fluid flow offshore Tumbes Basin, Peru. *Marine Geophysical Researches*, *38*(4), 409–423. https://doi.org/10.1007/s11001-017-9319-2

Ballas, G., Garziglia, S., Sultan, N., Pelleter, E., Toucanne, S., Marsset, T., et al. (2018). Influence of early diagenesis on geotechnical properties of clay sediments (Romania, Black Sea). *Engineering Geology*, *240*, 175–188. https://doi.org/10.1016/j.enggeo.2018.04.019

Bangs, N. L., Musgrave, R. J., & Tréhu, A. M. (2005). Upward shifts in the southern Hydrate Ridge gas hydrate stability zone following postglacial warming, offshore Oregon. *Journal of Geophysical Research*, *110*(B3). https://doi.org/10.1029/2004JB003293

Berndt, C., Bünz, S., Clayton, T., Mienert, J., & Saunders, M. (2004). Seismic character of bottom simulating reflectors: Examples from the mid-Norwegian margin. *Marine and Petroleum Geology*, *21*(6), 723–733. https://doi.org/10.1016/j.marpetgeo.2004.02.003

Colin, F., Ker, S., Riboulot, V., & Sultan, N. (2020). Irregular BSR: Evidence of an ongoing reequilibrium of a gas hydrate system. *Geophysical Research Letters*, *47*(20), e2020GL089906. https://doi.org/10.1029/2020GL089906

Davies, R. J., Maqueda, M. Á. M., Li, A., & Ganopolski, A. (2017). Millennial-scale shifts in the methane hydrate stability zone due to Quaternary climate change. *Geology*, *45*(11), 1027–1030. https://doi.org/10.1130/G39611.1

Davies, R. J., Maqueda, M. Á. M., Li, A., & Ireland, M. (2021). Climatically driven instability of marine methane hydrate along a canyon-incised continental margin. *Geology*, *49*(8), 973–977. https://doi.org/10.1130/G48638.1

Dickens, G. R., Castillo, M. M., & Walker, J. C. (1997). A blast of gas in the latest Paleocene: Simulating first-order effects of massive dissociation of oceanic methane hydrate. *Geology*, *25*(3), 259–262. https://doi.org/10.1130/0091-7613(1997)025<0259:ABOGIT>2.3.CO;2

Fabre, M. (2023). Files relative to model calculation and modelling results [Dataset]. *Zenodo*. https://doi.org/10.5281/zenodo.8417400

Geletti, R., & Busetti, M. (2011). A double bottom simulating reflector in the western Ross Sea, Antarctica. *Journal of Geophysical Research*, *116*(B4), B04101. https://doi.org/10.1029/2010JB007864

Haeckel, M., Bialas, J., Klaucke, I., Wallmann, K., Bohrmann, G., & Schwalenberg, K. (2015). Gas hydrate occurrences in the Black Sea–new observations from the German SUGAR project. *Fire in the Ice: Methane Hydrate Newsletter*, *15*(2), 6–9.

Han, S., Bangs, N. L., Hornbach, M. J., Pecher, I. A., Tobin, H. J., & Silver, E. A. (2021). The many double BSRs across the northern Hikurangi margin and their implications for subduction processes. *Earth and Planetary Science Letters*, *558*, 116743. https://doi.org/10.1016/j.epsl.2021.116743

Jahren, A. H., Arens, N. C., Sarmiento, G., Guerrero, J., & Amundson, R. (2001). Terrestrial record of methane hydrate dissociation in the Early Cretaceous. *Geology*, *29*(2), 159–162. https://doi.org/10.1130/0091-7613(2001)029<0159:TROMHD>2.0.CO;2

Jain, A. K., & Juanes, R. (2009). Preferential mode of gas invasion in sediments: Grain-scale mechanistic model of coupled multiphase fluid flow and sediment mechanics. *Journal of Geophysical Research*, *114*(B8). https://doi.org/10.1029/2008JB006002

Kennett, J. P., Cannariato, K. G., Hendy, I. L., & Behl, R. J. (2003). In *Methane hydrates in quaternary climate change: The clathrate gun hypothesis* (Vol. 54). Special Publications Series, American Geophysical Union.

Ker, S., Thomas, Y., Riboulot, V., Sultan, N., Bernard, C., Scalabrin, C., et al. (2019). Anomalously deep BSR related to a transient state of the gas hydrate system in the western Black Sea. *Geochemistry, Geophysics, Geosystems*, *20*(1), 442–459. https://doi.org/10.1029/2018GC007861

Major, C. O., Goldstein, S. L., Ryan, W. B., Lericolais, G., Piotrowski, A. M., & Hajdas, I. (2006). The co-evolution of Black Sea level and composition through the last deglaciation and its paleoclimatic significance. *Quaternary Science Reviews*, *25*(17–18), 2031–2047. https://doi.org/10.1016/j.quascirev.2006.01.032

Martinez-Lamas, R., Toucanne, S., Debret, M., Riboulot, V., Deloffre, J., Boissier, A., et al. (2020). Linking Danube River activity to Alpine Ice-Sheet fluctuations during the last glacial (ca. 33–17 ka BP): Insights into the continental signature of Heinrich Stadials. *Quaternary Science Reviews*, *229*, 106136. https://doi.org/10.1016/j.quascirev.2019.106136

Nimblett, J., & Ruppel, C. (2003). Permeability evolution during the formation of gas hydrates in marine sediments. *Journal of Geophysical Research*, *108*(B9). https://doi.org/10.1029/2001jb001650

Nisbet, E. G., & Piper, D. J. (1998). Giant submarine landslides. *Nature*, *392*(6674), 329–330. https://doi.org/10.1038/32765

Phrampus, B. J., & Hornbach, M. J. (2012). Recent changes to the Gulf Stream causing widespread gas hydrate destabilization. *Nature*, *490*(7421), 527–530. https://doi.org/10.1038/nature11528

Plaza-Faverola, A., Sultan, N., Lucchi, R. G., El bani Altuna, N., Ramachandran, H., Singhroha, S., et al. (2023). Spatial changes in gas transport and sediment stiffness influenced by regional stress: Observations from piezometer data along Vestnesa Ridge, eastern Fram Strait. *Journal of Geophysical Research: Solid Earth*, *128*(5), e2022JB025868. https://doi.org/10.1029/2022JB025868

Popescu, I., De Batist, M., Lericolais, G., Nouzé, H., Poort, J., Panin, N., et al. (2006). Multiple bottom-simulating reflections in the Black Sea: Potential proxies of past climate conditions. *Marine Geology*, *227*(3–4), 163–176. https://doi.org/10.1016/j.margeo.2005.12.006

Popescu, I., Lericolais, G., Panin, N., De Batist, M., & Gillet, H. (2007). Seismic expression of gas and gas hydrates across the western Black Sea. *Geo-Marine Letters*, *27*(2–4), 173–183. https://doi.org/10.1007/s00367-007-0068-0

Posewang, J., & Mienert, J. (1999). The enigma of double BSRs: Indicators for changes in the hydrate stability field? *Geo-Marine Letters*, *19*(1–2), 157–163. https://doi.org/10.1007/s003670050103

Riboulot, V., Cattaneo, A., Scalabrin, C., Gaillot, A., Jouet, G., Ballas, G., et al. (2017). Control of the geomorphology and gas hydrate extent on widespread gas emissions offshore Romania. *Bulletin de la Societe Geologique de France*, *188*(4), 26. https://doi.org/10.1051/bsgf/2017182

Riboulot, V., Ker, S., Sultan, N., Thomas, Y., Marsset, B., Scalabrin, C., et al. (2018). Freshwater lake to salt-water sea causing widespread hydrate dissociation in the Black Sea. *Nature Communications*, *9*(1), 117. https://doi.org/10.1038/s41467-017-02271-z

Riedel, M., Freudenthal, T., Bergenthal, M., Haeckel, M., Wallmann, K., Spangenberg, E., et al. (2020). Physical properties and core-log seismic integration from drilling at the Danube deep-sea fan, Black Sea. *Marine and Petroleum Geology*, *114*, 104192. https://doi.org/10.1016/j.marpetgeo.2019.104192

Ruppel, C., Dickens, G. R., Castellini, D. G., Gilhooly, W., & Lizarralde, D. (2005). Heat and salt inhibition of gas hydrate formation in the northern Gulf of Mexico. *Geophysical Research Letters*, *32*(4). https://doi.org/10.1029/2004GL021909

Ruppel, C. D., & Kessler, J. D. (2017). The interaction of climate change and methane hydrates. *Reviews of Geophysics*, *55*(1), 126–168. https://doi.org/10.1002/2016RG000534

Sloan, E. D., & Koh, C. A. (2007). *Clathrate hydrates of natural gases*. CRC press.

Somoza, L., Medialdea, T., & Gonzalez, F. J. (2022). Bottom simulating reflectors along the scan basin, a deep-sea gateway between the weddell sea (Antarctica) and scotia sea. *World Atlas of Submarine Gas Hydrates in Continental Margins*, 483–492. https://doi.org/10.1007/978-3-030-81186-0_41

Soulet, G., Delaygue, G., Vallet-Coulomb, C., Böttcher, M. E., Sonzogni, C., Lericolais, G., & Bard, E. (2010). Glacial hydrologic conditions in the Black Sea reconstructed using geochemical pore water profiles. *Earth and Planetary Science Letters*, *296*(1–2), 57–66. https://doi.org/10.1016/j.epsl.2010.04.045

Soulet, G., Ménot, G., Garreta, V., Rostek, F., Zaragosi, S., Lericolais, G., & Bard, E. (2011). Black Sea "lake" reservoir age evolution since the last glacial—Hydrologic and climatic implications. *Earth and Planetary Science Letters*, *308*(1–2), 245–258. https://doi.org/10.1016/j.epsl.2011.06.002

Srodon, J., & Eberl, D. D. (1984). Illite. *Reviews in Mineralogy and Geochemistry*, *13*(1), 495–544.

Starostenko, V. I., Rusakov, O. M., Shnyukov, E. F., Kobolev, V. P., & Kutas, R. I. (2010). Methane in the northern Black Sea: Characterization of its geomorphological and geological environments. *Geological Society, London, Special Publications*, *340*(1), 57–75. https://doi.org/10.1144/SP340.5

Sultan, N. (2007). Excess pore pressure and slope failures resulting from gas-hydrates dissociation and dissolution. In *Offshore technology conference*. OTC. OTC-18532). https://doi.org/10.4043/18532-MS

Sultan, N., Marsset, B., Ker, S., Marsset, T., Voisset, M., Vernant, A. M., et al. (2010). Hydrate dissolution as a potential mechanism for pockmark formation in the Niger delta. *Journal of Geophysical Research*, *115*(B8). https://doi.org/10.1029/2010JB007453

Thomas, Y., Marsset, B., Dupont, P., Ker, S., & Riboulot, V. (2023). Depth-migrated High Resolution seismic reflection profiles and interval velocity models in the western Black Sea [Dataset]. *Sea*. https://doi.org/10.17882/96701

Vasilev, A., Kozhuharov, E., Hristova, R., Botev, E., & Trendafilov, V. (2013). Gas hydrates study in Bulgaria.

Xu, W., & Ruppel, C. (1999). Predicting the occurrence, distribution, and evolution of methane gas hydrate in porous marine sediments. *Journal of Geophysical Research*, *104*(B3), 5081–5095. https://doi.org/10.1029/1998JB900092

Yefremova, A. G., & Zhizchenko, B. P. (1974). Occurrence of crystal hydrates of gases in the sediments of modern marine basins: Doklady akademii nauk SSSR (Vol. *214*).

References From the Supporting Information

Constantinescu, A. M., Toucanne, S., Dennielou, B., Jorry, S. J., Mulder, T., & Lericolais, G. (2015). Evolution of the Danube deep-sea fan since the last glacial maximum: New insights into Black Sea water-level fluctuations. *Marine Geology*, *367*, 50–68. https://doi.org/10.1016/j.margeo.2015.05.007

Erickson, A. J., & Von Herzen, R. P. (1978). Down-hole temperature measurements. *Deep Sea Drilling Project, Leg*, *42A*.

Goto, S., Yamano, M., & Kinoshita, M. (2005). Thermal response of sediment with vertical fluid flow to periodic temperature variation at the surface. *Journal of Geophysical Research*, *110*(B1). https://doi.org/10.1029/2004JB003419

Hillman, J. I., Burwicz, E., Zander, T., Bialas, J., Klaucke, I., Feldman, H., et al. (2018). Investigating a gas hydrate system in apparent disequilibrium in the Danube Fan, Black Sea. *Earth and Planetary Science Letters*, *502*, 1–11. https://doi.org/10.1016/j.epsl.2018.08.051

Ker, S., Marsset, B., Garziglia, S., Le Gonidec, Y., Gibert, D., Voisset, M., & Adamy, J. (2010). High-resolution seismic imaging in deep sea from a joint deep-towed/OBH reflection experiment: Application to a mass transport complex offshore Nigeria. *Geophysical Journal International*, *182*(3), 1524–1542. https://doi.org/10.1111/j.1365-246X.2010.04700.x

Marsset, B., Menut, E., Ker, S., Thomas, Y., Regnault, J. P., Leon, P., et al. (2014). Deep-towed high resolution multichannel seismic imaging. *Deep Sea Research Part I: Oceanographic Research Papers*, *93*, 83–90. https://doi.org/10.1016/j.dsr.2014.07.013

Soulet, G., Ménot, G., Bayon, G., Rostek, F., Ponzevera, E., Toucanne, S., et al. (2013). Abrupt drainage cycles of the Fennoscandian ice sheet. *Proceedings of the National Academy of Sciences*, *110*(17), 6682–6687. https://doi.org/10.1073/pnas.1214676110

Zander, T., Haeckel, M., Berndt, C., Chi, W. C., Klaucke, I., Bialas, J., et al. (2017). On the origin of multiple BSRs in the Danube deep-sea fan, Black Sea. *Earth and Planetary Science Letters*, *462*, 15–25. https://doi.org/10.1016/j.epsl.2017.01.006